

Electron emission from an individual, supported C_{60} molecule

M. E. Lin

Department of Physics, Purdue University, West Lafayette, Indiana 47907

R. P. Andres

School of Chemical Engineering, Purdue University, West Lafayette, Indiana 47907

R. Reifenberger

Department of Physics, Purdue University, West Lafayette, Indiana 47907

D. R. Huffman

Department of Physics, University of Arizona, Tucson, Arizona 85721

(Received 18 September 1991; revised manuscript received 3 September 1992)

The electron emission properties of a single C_{60} molecule supported on a W field-emission tip are reported. Using standard models, values for the size, effective work function, and desorption temperature of C_{60} were obtained. Energy distributions of electrons emitted from C_{60} exhibit a narrow two-peaked spectrum and indicate a splitting of the highest occupied molecular-orbital level.

I. INTRODUCTION

C_{60} molecules, detected by Kroto and co-workers,¹ have been the subject of intense interest since the success in purifying C_{60}/C_{70} from carbon soot produced using the Krätschmer-Huffman technique^{2,3} has made it possible to obtain sufficient material for detailed studies of this highly symmetric, self-assembled collection of 60 carbon atoms. Calculations of the properties of C_{60} have appeared⁴⁻⁸ and the spectroscopic features of C_{60} are being rapidly reported.⁹⁻¹⁴

The stability, symmetric shape, and small diameter of the C_{60} molecule make it a potentially interesting electron emission source. Due to its small diameter, electrons emitted from an individual supported C_{60} would form a bright source and produce an electron beam with small angular spread that would be useful in electron microscopy, holography, and interferometry.¹⁵⁻²⁰ Prior studies of electron emission from ultrasharp teton tips have demonstrated that the properties of the field emitted electron beam differ remarkably from those of beams emitted from conventional electron emission sources.^{21,22} The small radius of curvature of C_{60} suggests that a large electric-field enhancement can be achieved at the surface of the molecule, implying that electron emission through a supported C_{60} can be obtained without a measurable current from the surrounding substrate. The inert character of C_{60} also makes it an ideal candidate for a stable electron emission source since it will not become contaminated by adsorbed gas atoms. By placing the C_{60} molecule on the end of a field-emission tip, a particularly well-characterized scanning tunneling microscope (STM) tip could be fabricated. Such tips may ultimately find use as "standard tips" for intercomparison of STM data

between different laboratories. For all the reasons cited above, electron emission from an individual supported C_{60} is interesting. To perform such an experiment, however, techniques must be developed to capture a single C_{60} molecule and then study its electron emission properties.

Such an experiment is possible due to recent advances in the study of supported metal clusters. There has been considerable effort to learn more about the electronic and structural properties of supported clusters containing only a few hundred atoms since the properties of such clusters are expected to show a size dependence related to the confinement of electrons in a small three-dimensional structure. Historically, a fundamental limitation in many supported-cluster studies is the unknown distribution of particle sizes that inevitably occur in experimentally prepared cluster samples. This distribution in sizes, as well as the distribution in local environments, often obscures the essential size-dependent physics of interest. One way to circumvent this difficulty is to develop techniques sensitive to the properties of an individual cluster. In this way, any unwanted convolution produced by a spread in sizes can *a priori* be eliminated and the essential properties of the cluster under study can be probed. A number of experiments emphasizing this "individual cluster" approach has recently been reported.²³⁻²⁷

The present paper, utilizing these techniques developed for the study of individual nanometer-size supported metallic clusters, reports the electron emission properties of a single C_{60} supported on a W substrate. The remainder of this paper is organized in the following way. Following a short review of the experimental techniques used in this study, a brief theoretical section reviews the important concepts required to understand

the experimental results. Data on the electron emission characteristics of individual C_{60} are reported and interpreted using standard models of electron emission. Finally, a discussion of the significance of our results is provided.

II. EXPERIMENTAL CONSIDERATIONS

The Huffman-Krätschmer technique² was used to produce C_{60}/C_{70} dust containing $\sim 95\%$ C_{60} which proved to be a suitable starting material for our purposes. The C_{60}/C_{70} powder was loaded into a small quartz tube 13 mm long with a 2 mm inner diameter. This tube was inserted into a boron-nitride cylinder which was wrapped with two 0.25 mm diameter tungsten wires to form an oven. The temperature of the oven as a function of power delivered to the oven was calibrated to an accuracy of a few degrees beforehand in a separate vacuum chamber.

The oven was then mounted into an ultrahigh vacuum (UHV) chamber equipped with a 200 l/s differential ion pump and a titanium sublimator.²⁸ The oven was tilted $\sim 15^\circ$ with respect to a horizontal line and was positioned roughly 3 cm away from a tungsten tip formed by electrochemical etching W wire in a 1N NaOH solution. The tip was spot-welded onto a support loop fabricated from W wire. By passing current through the support loop, the tip could be raised to a given temperature in a controlled way. The tip assembly was then mounted on a flange equipped with a W/W-26% Re thermocouple (attached to the tip support loop) and an adjustable bellows to permit small three-dimensional movements of the tip. After the tip and oven were carefully aligned, standard UHV procedures were followed until the pressure in the chamber was reduced below 1.3×10^{-8} Pa (1×10^{-10} Torr).

It is well established that individual metallic clusters can be placed on a field emission tip and that they exhibit long-term stability in an UHV environment.^{25,29} We found that in order to successfully deposit a C_{60} molecule on the apex of a W tip, the W tip must be held at a positive bias voltage with respect to ground potential. Repeated experiments showed that when the temperature of the C_{60} oven had reached $\sim 420^\circ\text{C}$ for several minutes, at least one C_{60} could be successfully deposited on the tip provided the tip was biased at a positive voltage. On the contrary, if no voltage or a negative voltage was applied to a tip, no C_{60} could be captured. Instead, it appeared that the C_{60} were reflected off the tungsten tip, resulting in flashes emanating from a nearby fluorescent screen held at ground potential.

After a C_{60} was captured on the tip, a few thousand volts between the tip and the fluorescent screen produced a sufficient electric field to cause electrons to be drawn from the C_{60} molecule. These electrons were accelerated toward the 10 cm diameter screen and were visually observed as bright, circularly symmetric dots appearing on the screen. An idealized schematic of this process is shown in Fig. 1. After deposition, the tip was typically covered with between 1 and 5 C_{60} molecules. Normally, the required voltage to image C_{60} was about 3/4 to 4/5

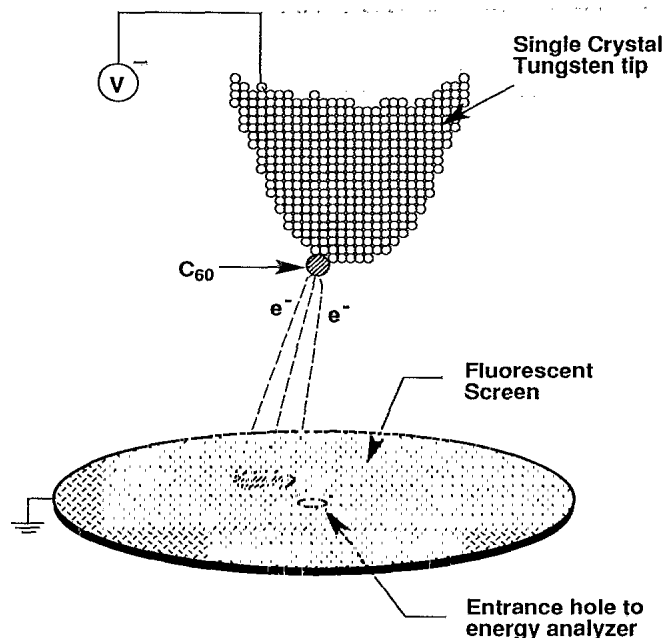


FIG. 1. A schematic of a C_{60} deposited on the end of a well-annealed tungsten field-emission tip. Electrons emitted from the C_{60} molecule strike a fluorescent screen and provide a highly magnified image of C_{60} . By steering the electrons into a probe hole, the distribution in energy of the emitted electron beam can be determined.

that required to image the clean W tip, a result consistent with the electric-field enhancement expected around a C_{60} cluster due to its small radius of curvature. After deposition, the supported C_{60} molecules were always found on the atomically rough surfaces of the tip rather than on the atomically flat facets that naturally develop on a well-annealed tip.

The magnitude of the emission current from a single C_{60} as a function of applied voltage was measured through an electrical feedthrough connected to the screen. Outside the chamber, a low light-level camera was positioned to observe the screen and was linked to a monitor and a video cassette recorder (VCR). Any light pattern produced by electrons striking the screen could be viewed on the monitor. In addition, the pattern could be recorded on tape using the VCR or digitized by a frame grabber for more quantitative analysis at a later time.

In the second phase of the study, a similar oven to that described above was placed inside a second vacuum chamber, operating at a pressure of less than 1.3×10^{-8} Pa (1×10^{-10} Torr). This chamber housed a field-emission electron-energy analyzer capable of resolving the distribution in energy of electrons emitted from an individual C_{60} . By depositing C_{60} clusters directly on the end of a W emitter as described above, electrons field emitted from an individual cluster could be collected and energy analyzed by a dispersive 127° analyzer known to have an energy resolution of 0.07 eV.³⁰ The details of this particular apparatus have been described elsewhere.³¹⁻³³ In this way, the energy spectra of electrons emitted could be measured as a function of an applied electric field.

III. THEORETICAL CONSIDERATIONS

The basic theory of field emission is based on the calculation of $j(E)$, the number of electrons of mass m emitted per unit area per unit time with energy between E and $E + dE$, due to an electric field F applied in the z direction.³⁴ The calculation of the distribution of emitted electrons requires an integration over all possible energies E and wave vectors $\mathbf{k} = (k_z, k_{\parallel})$:

$$j(E)dE = 2f(E) \int_E^{E+dE} \left(\frac{1}{\hbar} \frac{\partial E}{\partial k_z} \right) |T(k_z, E)|^2 \frac{d^3 k}{(2\pi)^3}. \quad (1)$$

In Eq. (1), $|T(k_z, E)|^2$, the transmission probability through the surface potential barrier, is usually evaluated for a metal with a Fermi level E_F and work function ϕ . The distribution of electrons is determined by the Fermi-Dirac function $f(E)$. The metal-vacuum interface is described in one dimension by an image rounded barrier given by

$$V(z) = \begin{cases} E_F + \phi - \frac{e^2}{4z} - eFz & \text{for } z > z_c, \\ 0 & \text{for } z < z_c, \end{cases}$$

where z_c is determined by $V(z_c) = 0$. Using the WKB approximation to estimate $T(k_z, E)$, the well-known free-electron result is obtained:

$$j_0(E) = \frac{md_E f(E)}{2\pi^2 \hbar^3} e^{-\frac{2}{\hbar} \left(\frac{2m}{\hbar^2} \right)^{\frac{1}{2}} \frac{(\phi + E_F - E)^{\frac{3}{2}}}{eF}} v(y), \quad (2)$$

where

$$\frac{1}{d_E} = 2 \left(\frac{2m}{\hbar^2} \right)^{\frac{1}{2}} \frac{(\phi + E_F - E)^{\frac{1}{2}}}{eF} t(y)$$

and $v(y)$, $t(y)$ are slowly varying, tabulated³⁵ functions of $y = (e^3 F)^{\frac{1}{2}} / (\phi)$. The shape and location of the field-emission energy distribution is shown in Fig. 2(a). The shape of $j_0(E)$ is roughly governed by the temperature of the emitter for $E > E_F$ and the transmission probability through the metal-vacuum barrier for $E < E_F$. An experimental measurement of this energy distribution involves further convolution of Eq. (2) with a symmetric Gaussian window function that accounts for the finite energy resolution of the energy analyzer. It is an experimental fact that Eq. (2) well describes the overall shape of the distribution of electrons emitted from field-emission tips fabricated from a variety of refractory metals.³⁴

Equation (2) can be further integrated to give the total current

$$J(F) = e \int_{-\infty}^{\infty} j_0(E) dE \\ = A' F^2 e^{-(B' \phi^{\frac{3}{2}} / F)}, \quad (3)$$

where A' and B' are known constants.³⁶ This result, known as the Fowler-Nordheim (F-N) equation, predicts a plot of $\ln[j(F)/F^2]$ vs $1/F$ will give a straight line with a slope related to the work function ϕ of the emitting

surface. Use of this equation has provided much of the systematic information now available on the work functions of the various faces of pure metals.

Now consider the case of electrons field emitted from an individual C_{60} . The expression for the emitted energy distribution will of course depend on the coupling of the C_{60} electronic wave functions to vacuum states propagating away from the C_{60} molecule. To solve this problem exactly is difficult, but a qualitative discussion suitable for our purposes can be presented within the framework outlined above. The major modification required is a proper account of the C_{60} electrons with a specific k_{\parallel} , a consequence of the hollow-shell geometry of the C_{60} molecule.

Under these circumstances, the variable of integration in Eq. (1) must be modified to permit summation over states with a fixed k_{\parallel} and can be written as³⁵

$$j(E)dE = \frac{\hbar}{2\pi^2 m} f(E) \int \int \rho(E, k_{\parallel}) \frac{|T(E, \mathbf{k}_{\parallel})|^2}{|1 + R(E, \mathbf{k}_{\parallel})|^2} d^2 k_{\parallel}. \quad (4)$$

The transmission probability for electrons with a specific

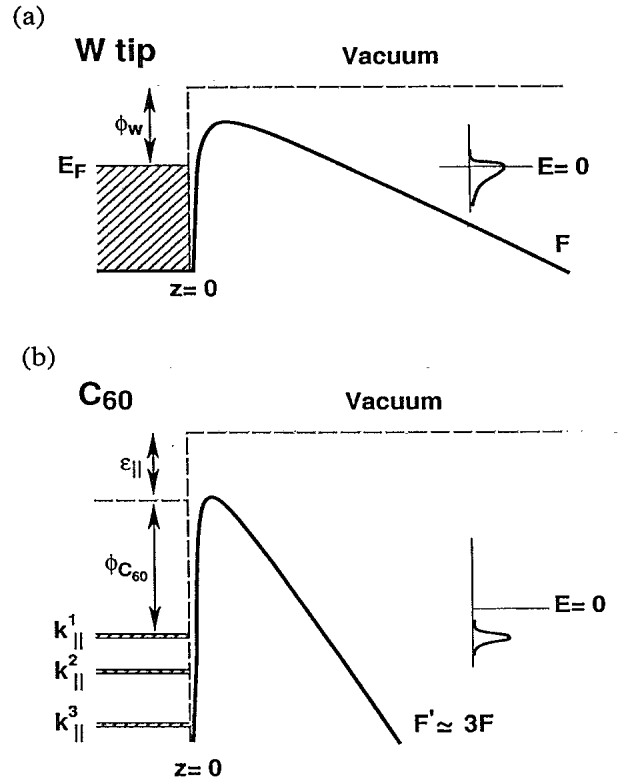


FIG. 2. (a) The image-rounded potential energy barrier and resulting energy distribution of electrons emitted from a tungsten tip. The work function ϕ and Fermi energy E_F of the metal substrate are indicated. (b) The modifications required for emission from C_{60} . The electric-field enhancement due to the small radius of the C_{60} molecule is indicated. The diagram shows a sequence of localized states with high k_{\parallel} . The height of the tunnel barrier must be increased by ϵ_{\parallel} as discussed in the text. In the example shown, the the highest occupied state dominates the emission current.

k_{\parallel} can be approximated by³⁵

$$T(E, k_{\parallel}) \simeq e^{\pi i/4} \sqrt{\eta} [1 + R(E, k_{\parallel})] \\ \times e^{-\frac{2}{3} \left(\frac{2m}{\hbar^2} \frac{2\eta}{E_F} \right) \left[\phi - E + E_F + \frac{\hbar^2 k_{\parallel}^2}{2m} \right]^{\frac{3}{2}}},$$

where

$$\eta = \left\{ \left(\frac{2m}{\hbar^2} \right) [\phi - E + E_F] + k_{\parallel}^2 \right\}^{\frac{1}{2}}, \\ \zeta = \left\{ \left(\frac{2m}{\hbar^2} \right) E + k_{\parallel}^2 \right\}^{\frac{1}{2}},$$

and

$$R(E, k_{\parallel}) \simeq \frac{\eta + i\zeta}{\eta - i\zeta}.$$

The quantity $\rho(E, k_{\parallel})$ in Eq. (4) is the average density of electrons at the surface of the C_{60} molecule with energy E and parallel momentum k_{\parallel} .

Even though the expression for the transmission coefficient contains k_{\parallel} in a complicated way, the argument of the exponent, which essentially controls the tunneling current, can be simplified by combining the parallel component of the electron's wave vector with the work function ϕ to yield an expression similar to Eq. (2) with the important exception that $\phi \rightarrow \phi + \epsilon_{\parallel}$ where

$$\epsilon_{\parallel} = \frac{\hbar^2 k_{\parallel}^2}{2m}. \quad (5)$$

It follows that Eq. (3) must also be modified in a similar way. It can be concluded from this discussion that expressions similar to those commonly used to describe electron emission from field-emission tips can be used to discuss electron emission from C_{60} , with the important exception that the value of ϕ obtained from a field-emission study of a single C_{60} must be interpreted as an "effective" work function. This modification is shown schematically in Fig. 2(b). Essentially, when discussing field emission for electron states with large k_{\parallel} using a one-dimensional model, the barrier height must be increased.

A second consideration appropriate for emission from C_{60} is the likelihood that the occupied k_{\parallel} closest to E_F of the substrate will dominate the emission current. Under these conditions, the integral in Eq. (4) can be replaced by a discrete sum. As a consequence, the observed energy distribution may contain discrete peaks (broadened by the energy resolution of the analyzer) located in the vicinity of the substrate E_F rather than a single continuous distribution of emitted electrons.

Another consideration appropriate for emission from a supported C_{60} is the evaluation of the electric field, F' , at the surface of the C_{60} . In principle, F' will be larger than the field, F , at the W substrate because of the smaller radius of curvature of the C_{60} molecule. In what follows, we assume F' can be related to F by geometrical considerations resulting from classical electrostatics, i.e., $F' = KF$.

By way of conclusion, after taking into account the modifications discussed above, it is possible to interpret

the field-induced emission from a supported C_{60} in terms of the standard model represented by Eqs. (2) and (3). Finally, it is worth pointing out that the above analysis assumes that k_{\parallel} is a good quantum number and hence is conserved during the emission process. Given the small diameter of the C_{60} molecule, this assumption may not hold true with the consequence that the one-dimensional approximation to the potential barrier may require revision.

IV. RESULTS

A. Electron emission from a single C_{60}

In a typical experiment, a sharp tungsten tip was first prepared in the usual way. After passing a sufficient current through the support loop to desorb gas from the tip, the well-known³⁷ twofold symmetric W field-emission pattern was observed when the tip was biased at -1900 V with respect to ground potential. During a successful C_{60} deposition, the voltage on the tip was set at $+900$ V while the oven temperature was maintained at ~ 420 °C for 5 min. The successful deposition of a C_{60} cluster could be confirmed by examining the field-emission pattern that resulted after the oven temperature was reduced to ambient. The success of a given deposition was sensitive to the tip's position relative to the oven, a result consistent with the collimated incoming flux of the C_{60} beam. Observations of cluster coverage vs deposition flux and of the size of the field-emission images provide good evidence that the individual objects captured on the field emitter are likely to be single C_{60} molecules rather than agglomerates comprised of many C_{60} molecules.

Electron emission from each supported C_{60} produced a bright spot on the fluorescent screen, a pattern quite distinct from the twofold symmetric pattern observed from a clean W tip. Emission from the C_{60} clusters consistently appeared at -1500 ± 100 V. Electron emission currents were measured as a function of applied voltage and currents $\sim 1 \times 10^{-9}$ A could be readily drawn from a single C_{60} cluster.

The field-emission pattern from C_{60} is highly symmetric as shown in Fig. 3 which is a digitized image of the intensity of light emanating from the fluorescent screen due to electrons emitted from an individual C_{60} . The electron current from a supported C_{60} was observed for time intervals up to a few hours, indicating a reasonably stable bonding configuration between C_{60} and the W substrate.

Internal structure above the background noise level is observed in these field-emission patterns. Careful examination revealed approximately 18 local peaks. It is tempting to associate these peaks with the location of atoms in the C_{60} structure, possibly enhanced by a charge transfer from the substrate to C_{60} as suggested by Chen *et al.*³⁸ Historically, it has been assumed that the resolution of a field-emission microscope is incapable of

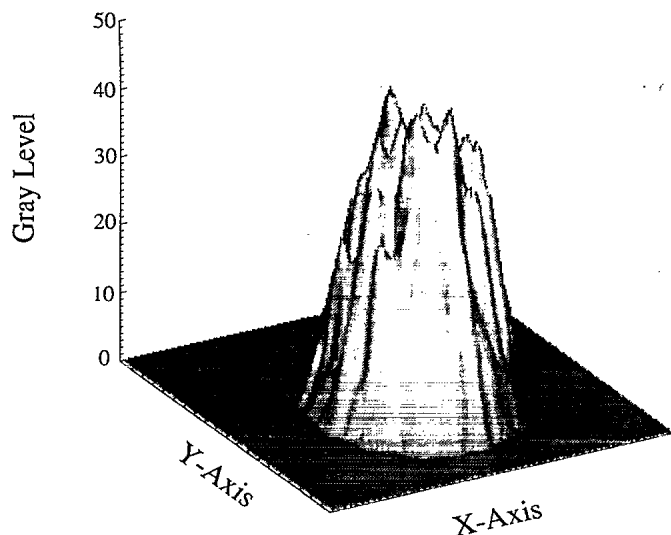


FIG. 3. A digitized image of the field emission pattern from C_{60} supported on a tungsten tip taken at -1600 V potential. The height of the emission pattern is related to the current density striking the fluorescent screen. The electron emission pattern is circular and characterized by a number of small secondary maxima.

imaging individual atoms. However, recent work by Binh *et al.*³⁹ using atomically sharp W microtips has demonstrated that atomic resolution from field emission may be possible. Although it is not clear what is the cause of the internal structure evident in Fig. 3, the possibility that we are imaging the individual carbon atoms or the covalent bonds between carbon atoms should not be dismissed at this time.

B. Desorption temperature of C_{60}

The ability of a C_{60} to bind to a substrate is a question of interest, and the observations performed during the course of these experiments give some information about the strength of this binding. In general, the binding of the C_{60} to W is relatively weak as compared to Au clusters on W tips.²⁴ An individual C_{60} did not stay on a W tip for more than 24 h while Au clusters can be studied for weeks at a time.

In Fig. 4, a typical sequence of F-N plots for an individual C_{60} as a function of substrate temperature is presented. Below 150°C no diffusion of the C_{60} over the W substrate was observed. When the substrate temperature was between 150°C and 200°C , the C_{60} rapidly desorbed as evidenced by the disappearance of the characteristic field-emission pattern from the molecule. As seen from Fig. 4, if the tip temperature was kept below 150°C , the field-emission I - V characteristics of C_{60} were stable and the slopes of subsequent F - N plots are roughly equal. Upon heating above 200°C , the C_{60} desorbed and the I - V characteristics represent the W tip. From this observation, it can be estimated that the binding energy between C_{60} and tungsten is of order $k_B T$, i.e., roughly equal to 35 meV. It should be realized that this estimate

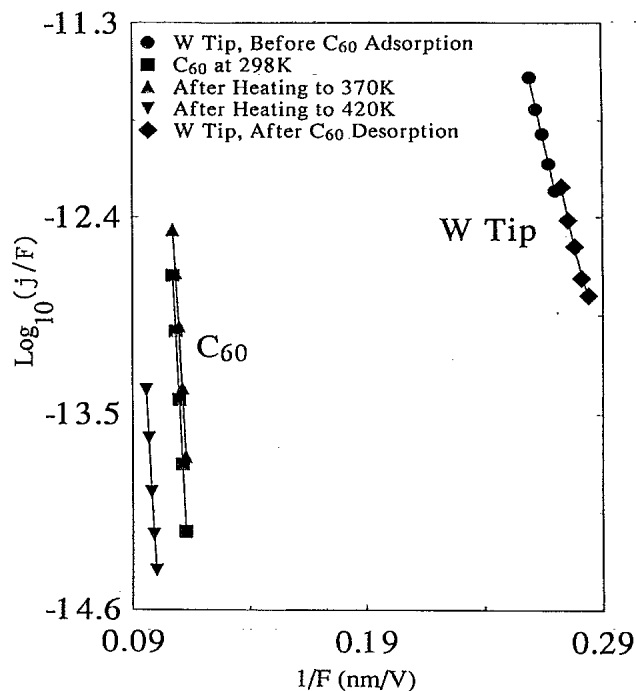


FIG. 4. Fowler-Nordheim plots of the electron emission current at ambient temperature from an individual C_{60} that has experienced different annealing temperatures. The Fowler-Nordheim plot for the W tip without a C_{60} molecule is also shown.

is for an isolated C_{60} supported on a W substrate, and may not be applicable to high coverage of C_{60} on W substrates.

C. Size of C_{60}

Direct evidence that we are observing electron emission from an individual C_{60} can be obtained from an estimate of the diameter of the object that produces the electron current. The electric-field strength at the W substrate, F is related to the voltage V applied to the tip by $F = \beta V$ where β is a geometrical factor related to the tip radius r_t by

$$r_t \approx \frac{1}{5\beta}. \quad (6)$$

From Fowler-Nordheim plots of the clean W tip, the geometrical factor, β of the tip can be estimated from Eq. (3) if an average work function for W of 4.5 eV is assumed. This yields a value of β of approximately $1.85 \times 10^4 \text{ cm}^{-1}$, and from Eq. (6) an estimate of the tip radius of 108 nm is obtained.

The size of the emitting C_{60} can now be approximately estimated from the diameter of its field emission image²⁸. Since there is a 10 cm separation between tip and screen, the magnification (M_0) of the microscope is roughly 9.2×10^5 from geometrical considerations alone. For electron emission from a small object on a field-emission tip, a magnification enhancement due to the

radius of curvature of the object must also be taken into account. The magnification (M) of the image of a small object must be modified such that^{25,40}

$$M \sim 1.1 \left(\frac{r_t}{r_c} \right)^{1/2} M_0, \quad (7)$$

where r_c is the radius of the emitting object. Measuring the radius of the C_{60} image on the fluorescent screen and substituting the radius into Eq. (7), the diameter of the emitting C_{60} is estimated to be 0.9 ± 0.4 nm. This rough estimate is consistent with both the diameter of a C_{60} cage which is 0.7 nm and the van der Waals diameter of the C_{60} molecule which is 1.0 nm. At the present time, it is not clear which diameter is most appropriate to compare with our data and further clarification of this issue may hold the key to precise calibration of field-emission images in the future.

D. Effective work function of C_{60}

From the F - N plots of Fig. 4, the effective work function of C_{60} can also be estimated²⁵. From Eq. (2), it follows that

$$\frac{\phi_{C_{60}}^{3/2}}{K \beta m_{C_{60}}} = \frac{\phi_W^{3/2}}{\beta m_W}, \quad (8)$$

where m_W and $m_{C_{60}}$ are the F - N slopes for the clean W tip and from the C_{60} cluster, respectively, and K is the electric-field enhancement factor related to the finite radius of C_{60} . Assuming the structure of C_{60} to be spherical, a reasonable value of $K = 3$ can be calculated from classical electrostatic arguments. Using the F - N slopes obtained from Fig. 4 and this value for K , the effective work function of C_{60} is found to be 11.7 ± 0.5 eV. This value of ϕ is quite high, since work functions for most refractory metals range between 4.5 and 5.5 eV. The large value of ϕ obtained in this manner is thought to result from the large parallel component of the electron's wave function as described in Sec. III above.

It should be noted that the value of ϕ obtained above is close to the effective potential barrier commonly used in STM studies of highly oriented pyrolytic graphite⁴¹ that is comprised of two-dimensional carbon planes. Also, even though the second ionization energy of C_{60} is around 12 eV, the electrons we measure are not emitted from a positively charged C_{60} since electron emission through the resulting Coulomb barrier is not possible under the conditions of our experiment.

E. Energy distribution of electrons emitted from C_{60}

Using the energy analyzer described in Sec. II above, the energy distribution of electrons emitted from a single C_{60} was also measured. The results are shown in Fig. 5 which is a logarithmic plot of the number of electrons emitted from C_{60} as a function of energy. For the purposes of comparison, the energy distribution of electrons emitted from a clean W substrate (this data was taken

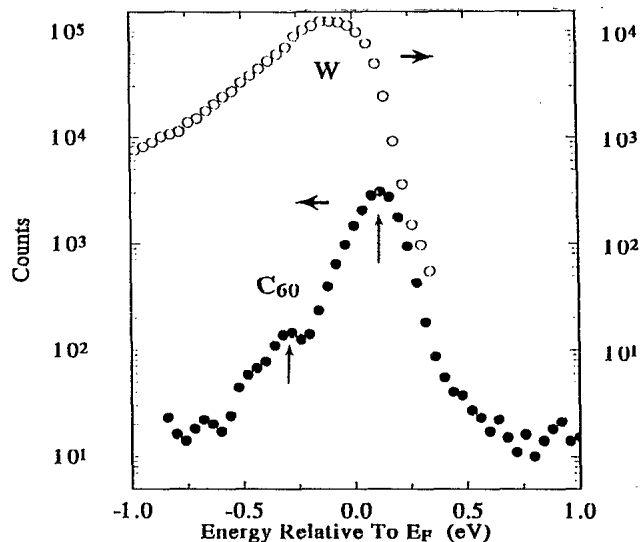


FIG. 5. The energy distribution from an individual C_{60} plotted on a logarithmic scale. The vertical arrows mark the position in energy of the two peaks observed in the C_{60} energy distribution. The energy distribution from a clean W tip obtained after desorbing the C_{60} molecule is also shown.

after the C_{60} molecule was desorbed) is also shown. The data from C_{60} shows a substantially narrower energy distribution with a full width at half maximum (FWHM) ~ 0.18 eV, about a factor of 2 smaller than observed for clean W . Surprisingly, the peak in the C_{60} distribution is shifted ~ 0.13 eV above E_F of the W substrate and indicates that the electronic states responsible for electron emission are not pinned to the substrate Fermi level.

In addition to the major peak, a second minor peak is observed at an energy of ~ 0.3 eV below the substrate E_F . Figure 6 shows how the shape of the electron-energy distribution evolves as the electric field is increased. A gradual broadening is observed that is consistent with a decrease in the barrier width with increasing electric field, resulting in an increased transmission probability. The rapid decrease in the transmission probability with decreasing energy only permits studies of the highest filled states using the field-emission technique.

A slight shift (~ 0.4 meV/V) of the major peak position to lower energy with increasing applied voltage is also observed. This result is characteristic of electron emission from small structures and is qualitatively consistent with the observation that peaks in the energy distribution of electrons emitted from nanometer-size Au clusters also shift to lower energies with increasing electric field.^{42,43} At the present time, this shift can be studied only over a small range of applied voltages due to the exponential increase in field emission current with applied voltage.

The ~ 0.43 eV splitting in the electron-energy distribution measured by field emission in this study is different from the splitting observed in UV photoemission studies of C_{60} thin films reported by Lichtenberger *et al.*^{44,45} or with the synchrotron photoemission data obtained by Weaver *et al.*¹³ An important difference between these

two studies and the one reported here is substrate coverage. The photoemission studies involve electron emission from films of C_{60} adsorbed onto substrates while the data reported here result from only *one* C_{60} . Also, in the case of the synchrotron photoemission study, the energy resolution was ~ 0.2 eV, making it difficult to resolve the size of the splitting observed here. A quantitative explanation for the splitting observed in this study may require a proper account of the applied electric field (typically $F' \approx 5 \times 10^9$ V/m) which may be strong enough to break the degeneracy of the highest occupied molecular-orbital (HOMO) h_u level. This high electric field is required to produce field emission, but it also could break the symmetry of the h_u energy level which is fivefold degenerate. Further calculation of the magnitude of this splitting is required in order to determine if this effect offers a possible explanation of our data. Another possibility is that the C_{60} -W interaction results in a distortion of the molecule, which produces an additional splitting of the highest filled states.

The emission of electrons from a state located ~ 0.13

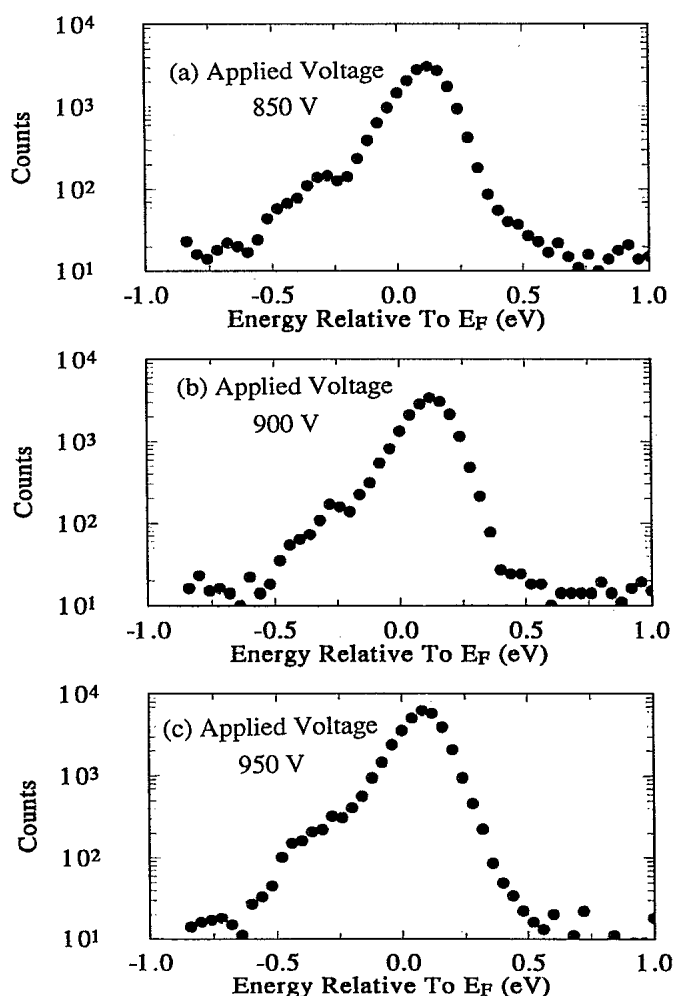


FIG. 6. The electric-field dependence of the energy distribution from a single C_{60} molecule. The distributions show a broadening as the electric field increases, a consequence of the decrease in the width of the potential barrier with increasing electric field.

eV above E_F of the substrate is surprising and may indicate a thermal broadening mechanism for electrons injected from the tip into the C_{60} molecule. Since the tip is at room temperature, the expected thermal broadening of the Fermi-Dirac distribution function can provide a supply of electrons at energies a few $k_B T$ above E_F . These electrons could in turn resonantly tunnel through C_{60} states a few $k_B T$ above the Fermi level of the tip with a significantly higher transmission probability because of the exponential dependence of transmission with energy. Alternatively, heating of the cluster by injection of electrons from the tip is also possible. Such a thermoelectric effect has recently been discussed in conjunction with the heating of small tunnel junctions and may cause a significant increase in the temperature of the C_{60} molecule above ambient.⁴⁶

V. DISCUSSION AND CONCLUSIONS

The electron emission properties of an individual C_{60} molecule supported on a W substrate have been studied using field-emission techniques. Electrons emitted from C_{60} are found to produce a highly symmetric field emission pattern that contains secondary structure that may be related to enhanced electron emission from specific regions on the surface of the C_{60} molecule. The electron emission is stable over long periods of time and little or no change in position of the C_{60} molecule is observed, indicating a reasonably stable bond between a single C_{60} and an atomically clean W substrate. Desorption measurements show that the C_{60} is rapidly desorbed from the W tip at temperatures above 150°C . A study of the electric-field dependence of the field-emission current reveals an anomalously high value for the C_{60} work function, a result that is tentatively explained by the two-dimensional nature of the electron states of C_{60} . Finally, energy distributions of the electrons emitted from an individual C_{60} are reported. These reveal a narrow distribution of emitted electrons, and show two features that are thought to be related to the electric-field splitting of the HOMO h_u level in C_{60} .

The most important conclusion obtained from this initial study is that in an electric field of $\sim 3 \times 10^9$ V/m, a single C_{60} emits an intense beam of electrons having a narrow energy distribution. This fact, coupled with the positional stability of the C_{60} molecule on the W tip, indicates that a suitably doped C_{60} may ultimately prove to be an easily fabricated, stable, subnanometer electron emission source.

ACKNOWLEDGMENTS

The authors would like to thank D.L. Lichtenberger for helpful comments during the preparation of this manuscript. This work was partially supported by the U.S. DOE Contract DE-FG02-88ER45162. M.E. Lin thanks the David Ross Foundation for financial support during the course of this work. One of us (R.R.) would like to thank N. Garcia for an illuminating discussion on the importance of heating effects in small tunnel junctions prior to publication.

- ¹H.W. Kroto, J.R. Heath, S.C. O'Brien, R.F. Curl, and R.E. Smalley, *Nature* **318**, 162 (1985).
- ²W. Krätschmer, L.D. Lamb, K. Fostiropoulos, and D.R. Huffman, *Nature* **347**, 354 (1990).
- ³G. Meijer and D.S. Bethune, *Chem. Phys. Lett.* **175**, 1 (1990).
- ⁴R.C. Haddon, L.E. Brus, and K. Raghavachari, *Chem. Phys. Lett.* **125**, 459 (1986).
- ⁵S. Satpathy, *Chem. Phys. Lett.* **130**, 545 (1986).
- ⁶R.E. Stanton and M.D. Newton, *J. Phys. Chem.* **92**, 2141 (1988).
- ⁷Z. Slanina, J.M. Rudzinski, M. Togasi, and E. Osawa, *J. Mol. Struct. (Theochem)* **202**, 169 (1989).
- ⁸W.G. Harter and D.E. Weeks, *J. Chem. Phys.* **90**, 4727 (1989).
- ⁹S.C. O'Brien, J.R. Heath, R.F. Curl, and R.E. Smalley, *J. Chem. Phys.* **88**, 220 (1988).
- ¹⁰P.P. Radi, M.T. Hsu, M.E. Rincon, P.R. Kemper, and M.T. Bowers, *Chem. Phys. Lett.* **174**, 223 (1990).
- ¹¹W. Krätschmer, K. Fostiropoulos, and D.R. Huffman, *Chem. Phys. Lett.* **170**, 167 (1990).
- ¹²D.S. Bethune, G. Meijer, W.C. Tang, and H.J. Rosen, *Chem. Phys. Lett.* **174**, 219 (1990).
- ¹³J.H. Weaver, J.L. Martins, T. Komeda, Y. Chen, T.R. Ohno, G.H. Kroll, N. Troullier, R.E. Haufler, and R.E. Smalley, *Phys. Rev. Lett.* **66**, 1741 (1992).
- ¹⁴Y.Z. Li, J.C. Patrin, M. Chander, J.H. Weaver, L.P.F. Chibante, and R.E. Smalley, *Science* **252**, 547 (1991).
- ¹⁵A. Tonomura, *Rev. Mod. Phys.* **59**, 639 (1987).
- ¹⁶H. Lichte, *Ultramicroscopy* **20**, 293 (1986).
- ¹⁷F.G. Missiroli, G. Pozzi, and U. Valdre, *J. Phys. E* **14**, 649 (1981).
- ¹⁸N. Garcia and H. Rohrer, *J. Phys. Condens. Matter* **1**, 3737 (1989).
- ¹⁹P. Serena, L. Escapa, J.J. Saenz, N. Garcia, and H. Rohrer, *J. Microsc.* **152**, 355 (1988).
- ²⁰H.-W. Fink, *IBM J. Res. Dev.* **30**, 460 (1986).
- ²¹Vu Thien Binh and J. Marien, *Surf. Sci.* **102**, L539 (1988).
- ²²Vu Thien Binh, *J. Microsc.* **152**, 355 (1988).
- ²³T. Castro, Y.Z. Li, R. Reifengerger, E. Choi, S.B. Park, and R.P. Andres, *J. Vac. Sci. Technol. A* **7**, 2845 (1989).
- ²⁴T. Castro, R. Reifengerger, E. Choi, and R.P. Andres, *Surf. Sci.* **234**, 43 (1990).
- ²⁵T. Castro, R. Reifengerger, E. Choi, and R.P. Andres, *Phys. Rev. B* **42**, 8548 (1990).
- ²⁶Y.Z. Li, R. Reifengerger, E. Choi, and R.P. Andres, *Surf. Sci.* **250**, 1 (1991).
- ²⁷T. Castro, E. Choi, Y.Z. Li, R.P. Andres, and R. Reifengerger, in *Clusters and Cluster-Assembled Materials*, edited by R.S. Averback, J. Bernholc, and D.L. Nelson, MRS Symposia Proceedings No. 206 (Materials Research Society, Pittsburgh, 1991), p. 159.
- ²⁸Tom K. Castro, Ph.D. thesis, Purdue University, 1989.
- ²⁹M.E. Lin, R.P. Andres, and R. Reifengerger, *Phys. Rev. Lett.* **67**, 477 (1991).
- ³⁰Y. Gao, R. Reifengerger, and R.M. Kramer, *J. Phys. E* **18**, 381 (1985).
- ³¹Y. Gao and R. Reifengerger, *Phys. Rev. B* **35**, 6627 (1987).
- ³²Y. Gao and R. Reifengerger, *Phys. Rev. B* **35**, 4284 (1987).
- ³³Y. Gao and R. Reifengerger, *Phys. Rev. B* **35**, 8301 (1987).
- ³⁴J.W. Gadzuk and E.W. Plummer, *Rev. Mod. Phys.* **43**, 487 (1973).
- ³⁵A. Modinos, *Field, Thermionic and Secondary Electron Emission Spectroscopy* (Plenum, New York, 1984).
- ³⁶R.H. Fowler and L.W. Nordheim, *Proc. R. Soc. London Ser. A* **119**, 173 (1928).
- ³⁷R.H. Good and E.W. Müller, in *Handbuch der Physik*, 2nd ed. (Springer-Verlag, Berlin, 1956), Vol. 2, p. 176.
- ³⁸T. Chen, S. Howells, M. Gallagher, L. Yi, D. Sarid, D.L. Lichtenberger, K.W. Nebesny, and C.D. Ray, in *Clusters and Cluster-Assembled Materials* (Ref. 27), p. 721.
- ³⁹J.J. Saenz, N. Garcia, H. De Raedt, and Vu Thien Binh, *J. Phys. (Paris) Colloq.* **50**, C8 (1989).
- ⁴⁰D.J. Rose, *J. Appl. Phys.* **27**, 215 (1956).
- ⁴¹A.M. Baro, A. Bartolome, L. Vazquez, N. Garcia, R. Reifengerger, E. Choi, and R.P. Andres, *Appl. Phys. Lett.* **51**, 1594 (1987).
- ⁴²M.E. Lin, R. Reifengerger, and R.P. Andres, *Phys. Rev. B* **46**, 15490 (1992).
- ⁴³M.E. Lin, R. Reifengerger, A. Ramachandra, and R.P. Andres, *Phys. Rev. B* **46**, 15498 (1992).
- ⁴⁴D.L. Lichtenberger, K.W. Nebesny, C.D. Ray, D.R. Huffman, and L.D. Lamb, *Chem. Phys. Lett.* **176**, 203 (1991).
- ⁴⁵D.L. Lichtenberger, M.E. Jatcko, K.W. Nebesny, C.D. Ray, D.R. Huffman, and L.D. Lamb, in *Cluster and Cluster-Assembled Materials* (Ref. 27), p. 673.
- ⁴⁶N. Garcia and F. Guinea, *Phys. Rev. B* **46**, 571 (1992).